A New and Easy Method for Making Ni and Cu Microtubules and Their Regularly Assembled Structures

Chien-Chung Han,* Meng-Yi Bai, and Jyh-Tsung Lee

Department of Chemistry, National Tsing Hua University, Hsinchu, Taiwan, ROC

Received April 13, 2001. Revised Manuscript Received August 14, 2001

Ni and Cu microtubules of several centimeters in length can be easily prepared using a new method herewith by the pyrolysis of composite fibers consisting of a poly(ethylene terephthalate) (PET) core fiber and an electroless-plated metal skin layer. Through the use of this approach, the diameter, wall-thickness, and length of metal microtubules can be conveniently controlled. Various analytical methods, including scanning electron microscopy, transmission electron microscopy, X-ray diffraction analysis, and electron paramagnetic resonance, were used to characterize the resultant metal microtubules. The results indicated that the Ni microtubules essentially consist of single crystalline fcc-Ni, with the normal of the {110} planes being parallel to the direction of the tube axis, whereas the resultant Cu microtubules are polycrystalline. The respective conductivities for the resultant Ni and Cu microtubules were 1.22×10^5 (±20%) S/cm and $>1.58 \times 10^5$ (±25%) S/cm, quite similar to those of pure metals. Most interestingly, this method also provides a feasible approach for the preparation of two- or three-dimensional well-organized metal microtubular assemblies from suitable woven fabrics or structures.

Introduction

Metal microtubules have recently caused a great deal of research interest in the chemistry, physics, and material science fields,[1] because of their interesting properties and potentials in applications such as porous electrodes for flow electrolysis,[2a] microring electrodes,[2b] ion-transport selections,[3] quantum devices,[4a] memory devices,[4b] through-hole plating,[4c] and catalytic microreactors.[5] To date, several metal thin-film deposition methods have been reported for the fabrication of metal microtubules, such as the use of plasma-enhanced physical and chemical vapor deposition (PEPVD and PECVD) and conventional CVD to deposit metal coating onto monofilament polyester fibers that were individually held between two arms of a rotating headset to ensure complete and even coating coverage of the filament surface.[1o] Furthermore, various templates, including the microporous polycarbonate or alumina membrane,[1a−e] lipid tubules,[1f−g] self-assembled microtubules of diacetylenic lipid,[1h−j] protein fibers,[1k−l] and carbon nanotubes,[1m] have been employed, in conjugation with electrochemical or electroless plating, to prepare microtubules of several micrometers in length. However, these fabrication methods are complicated and costly because they involve the use of either magnetron sputtering systems[1o] or electrochemical cells,[1a−d] or complicatedly prepared templates of limited sizes (in terms of thickness/length, or area).[1a−m] Recently, we have successfully prepared micrometer-sized carbon tubes[6] from the pyrolysis of a composite fiber that contains a thermally more stable skin layer, such as polypyrrole, and a thermally less stable core template, such as poly(ethylene terephthalate) (PET) fiber. After appropriate pyrolysis treatment, the PET core of the composite fiber was thermally degraded and mostly volatilized, meanwhile the polypyrrole skin layer was carbonized and left as a hollow carbon tube. It is obvious that the same idea could be applied to fabricate microtubules composing of other materials, with metals being evident candidates. In this work, we report this easy, feasible, and highly scalable method for fabricating Ni

* To whom correspondence should be addressed. Tel: 886-3-5724998. Fax: 886-3-5711082. E-mail: cchan@mx.nthu.edu.tw.

(1) (a) Brumlik, C. J.; Martin, C. R. *J. Am. Chem. Soc.* **1991**, *113*, 3174. (b) Brumlik, C. J.; Menon, V. P. V.; Martin, C. R. *J. Mater. Res.* **1994**, *9*, 1174. (c) Tierney, M. J.; Martin, C. R. *J. Phys. Chem.* **1989**, *93*, 2878. (d) Penner, R. M.; Martin, C. R. *Anal. Chem.* **1987**, *59*, 2625. (e) Fischer, B. E.; Spohr, R. *Rev. Mod. Phys.* **1983**, *55*, 907. (f) Schnur, J. M. *Science* **1993**, *262*, 1669−1676. (g) Schnur, J. M.; Shashidhar, R. *Adv. Mater.* **1994**, *6*, 971−974. (h) Chow, G. M.; Stockton, W. B.; Price, R.; Baral, S.; Ting, A. C.; Ratna, B. R.; Shoen, P. E.; Schnur, J. M.; Bergeron, G. L.; Czarnaski, M. A.; Hickman, J. J.; Kirkpatrick, D. A. *Mater. Sci. Eng.* **1992**, *A158*, 1. (i) Wang, G.; Hollingsworth, R. I. *Langmuir* **1999**, *15*, 6135−6138. (j) Markowitz, M.; Baral, S.; Brandow, S.; Singh, A. *Thin Solid Films* **1993**, *224*, 242−247. (k) Mertig, M.; Kirsch, R.; Pompe, W. *Appl. Phys.* **1998**, *66*, S723−S727. (l) Kirsch, R.; Mertig, M.; Pompe, W.; Wahl, R.; Sadowski, G.; Böhm, K. J.; Unger, E. *Thin Solid Films* **1997**, *305*, 248−253. (m) Ang, L. M.; Hor, T. S. A.; Xu, G. Q.; Tung, C. H.; Zhao, S. P.; Wang, J. L. S. *Carbon* **2000**, *38*, 363−372. (n) Jiang, J. Z.; Nielsen, K. F.; Kragh, F.; Gerward, L.; Bohr, J. *J. Mater. Sci. Lett.* **1998**, *17*, 1301−1303. (o) Fox, G. R. *J. Mater. Sci. Lett.* **1995**, *14*, 1496.

(2) (a) Bard, A. J.; Faulkner, L. R. *Electrochemical Methods: Fundamentals and Applications*, 1st ed.; John Wiley & Sons: New York, 1980; p 401. (b) Fleischmann, M.; Bandyopadyay, S.; Pons, S. *J. Phys. Chem.* **1985**, *89*, 5537.

(3) (a) Nishizawa, M.; Menon, V. P.; Martin, C. R. *Science* **1995**, *268*, 700. (b) Lee, S. B.; Martin, C. R. *Anal. Chem.* **2001**, *73*, 768−775. (c) Martin, C. R.; Nishizawa, M.; Jirage, K.; Kang, M. *J. Phys. Chem. B* **2001**, *105*, 1925−1934.

(4) (a) Randall, J. N.; Reed, M. A.; Frazier, G. A. *J. Vac. Sci. Technol.* **1989**, *B7*, 1398. (b) Oro, J. A.; Wolfe, J. C. *J. Vac. Sci. Technol.* **1983**, *B1*, 1088. (c) Hazlebeck, D. A.; Talbot, J. B. *J. Electochem. Soc.* **1991**, *138*, 1998.

(5) Yu, X.; Li, H.; Deng, J. F. *Appl. Catal. A* **2000**, *199*, 191.

(6) (a) Han, C. C.; Lee, J. T.; Yang, R. W.; Chang, H.; Han, C. H. *Chem. Commun.* **1998**, 2087. (b) Han, C. C.; Lee, J. T.; Yang, R. W.; Chang, H.; Han, C. H. *Chem. Mater.* **1999**, *11*, 1806.

10.1021/cm0103287 CCC: $20.00
Published on Web 10/12/2001

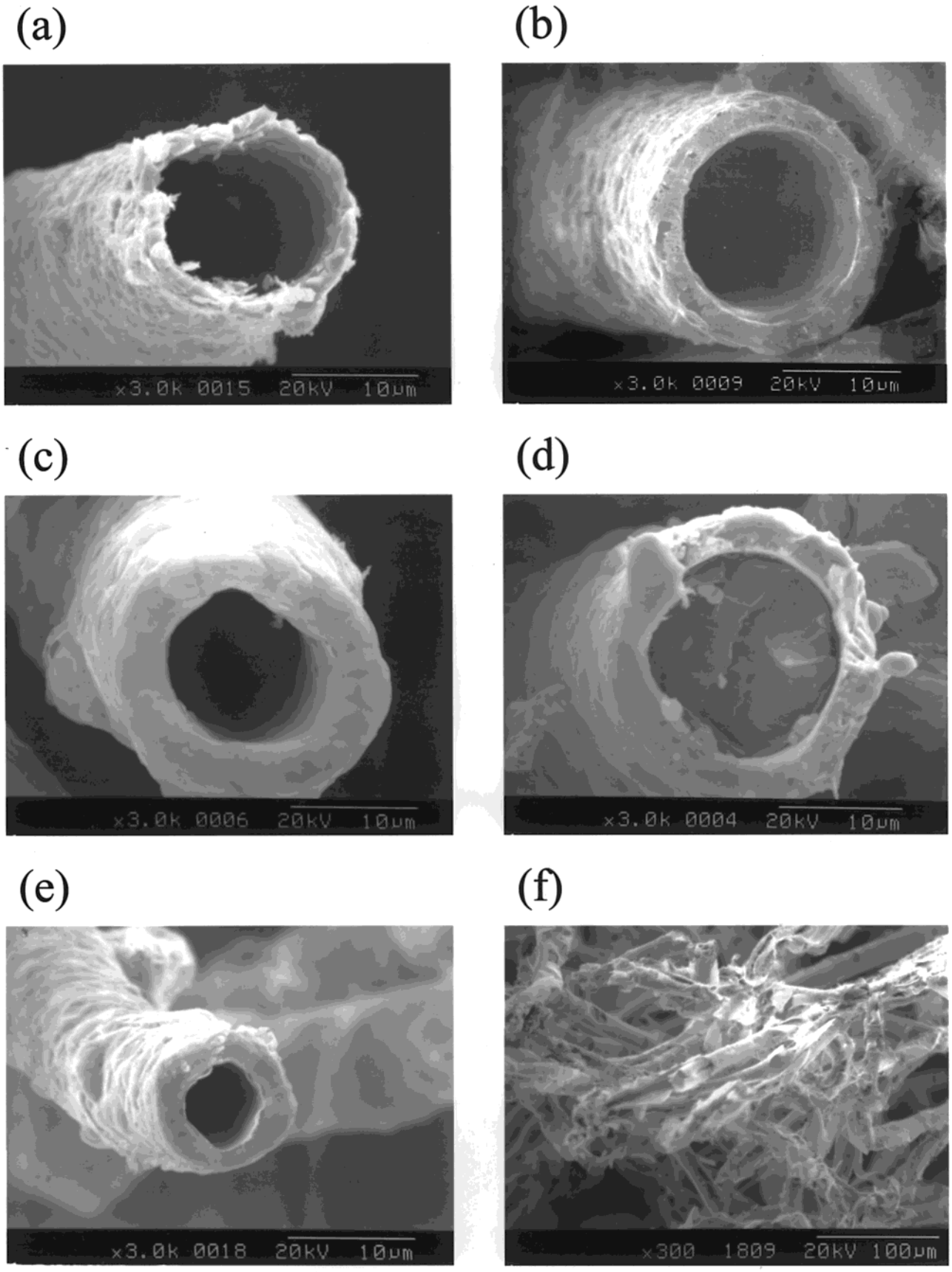

Figure 1. SEM micrographs for Ni microtubules of ca. 16 μm in diameter as prepared from their corresponding Ni/PET composite fibers that had been electroless-plated for (a) one, (b) two, and (c) three cycles; (d) the parent Ni/PET composite fiber for the Ni microtubules in (c); (e) Ni microtubules of ca. 7μm in diameter; (f) Ni microtubules of ca. 16 μm in diameter resulted from the Ni/PET composite fibers that had been electroless-plated for one cycle under the same conditions as those for the parent composite fiber of (a), except that twice the amount of PET fiber was employed as the plating template.

and Cu metal microtubules via the pyrolysis of the composite fibers consisting of a metal skin layer and a PET core.

Experimental Section

Materials. The PET yarns containing ca. 180 filaments in each fiber bundle were obtained from Far Eastern Textile Co. Ltd. (Taiwan) or Union Chemical Laboratories, Industrial Technology Research Institute (Taiwan). The average diameter of each PET filament was ca. 16.7 or 7 μm. The resistance of the deionized water used for experiments was 18.2−18.3 MΩ. Stannous chloride (Strem Chemical Inc., 98%), hydrochloric acid (J. T. Baker, 36.5−38%), palladium chloride (Aldrich, 99%), nickel sulfate (Aldrich, 99%), sodium acetate (Aldrich, 99%), glacial acetic acid (TEDIA, HPLC/Spectro), sodium hypophosphite (Aldrich, 99%), copper sulfate (Aldrich, 98%), the tetrasodium salt of EDTA (Showa Chemicals Inc., 99%), sodium hydroxide (Riedel-de Haen, ACS grade), and formaldehyde (37 wt % aqueous solution, Aldrich) were used as purchased.

The metal microtubules were prepared from metal-plated PET fibers via thermal treatment under a stream of N_2 (0.5 L/min) in a quartz tube oven by first heating from room temperature (rt) to 400 °C at 5 °C/min and then holding at 400 °C for 30 min, followed by heating to 800 °C at 10 °C/min and then holding at 800 °C for 3 h, before cooling naturally to rt. The resultant Ni microtubules may contain some residual carbon on the inner surface (possibly originated from the PET core), which can be easily removed by heating at 800 °C for 1−3 h under a reducing atmosphere, such as one provided by a 1:9 mixture (v/v) of H_2/N_2. The metal platings were formed by the typical electroless-plating method as reported in the literature with slight modifications.[7a−b] The PET fibers (0.125 g) were first sensitized by a 30 min immersion with 50 mL $SnCl_2$ aqueous solution (0.0053 M for Ni plating; 0.1 M for Cu plating) that contained 0.01 M HCl and then activated by another 30 min immersion with 50 mL $PdCl_2$ aqueous solution (0.0028 M for Ni plating; and 0.01 M for Cu plating) containing 0.01 M HCl, before being soaked in the corresponding Ni or Cu plating solution. The Ni plating was performed at 50 °C by the single addition of aqueous sodium hypophosphite solution (0.5 mL, 20 M) as a reductant to the Ni-plating solution (50 mL); whereas the Cu plating was performed at rt by a slow addition (with a syringe pump at 3.05 mL/h) of 1.52 mL of 37 wt % aqueous formaldehyde solution as a reductant to the Cu-plating solution (50 mL). After the addition of the respective reductant solution, the Ni plating was allowed to proceed for 1.5 h, while the Cu plating was allowed to proceed for 30 min. The thickness of the metal skin layer could be further controlled by employing multiple cycles of plating treatment. The detailed electroless-plating bath compositions are described below:

Ni Plating Bath. Nickel sulfate hexahydrate (1.314 g, 5 mmol) and sodium acetate (1.641 g, 20 mmol) were dissolved in deionized water (50 mL). The pH of the resultant metal-plating solution was adjusted to 6 by the addition of glacial acetic acid, and then the solution was heated to 50 °C before use.

Cu Plating Bath. Copper sulfate pentahydrate (0.499 g, 2 mmol), the tetrasodium salt of EDTA tetrahydrate (2.075 g, 4.5 mmol), and sodium hydroxide (0.7 g, 0.0175 mol) were dissolved in deionized water (50 mL) with ultrasonic agitation to result in a clear blue solution.

Instrumentation. The morphology and shape of the resultant metal microtubules were observed by scanning electron microscopy (SEM) on a Hitachi S-2300 microscope or by field emission scanning electron microscopy (FESEM) using Hitachi S-4000 equipment, both using an accelerating voltage of 20 kV. The surface of samples was coated with a thin film of Pt/Pd or Au (thickness ca. 100−200 Å) for SEM observations. The X-ray powder diffraction for the ground-up metal microtubules was obtained by a Shimadzu XD-5 X-ray diffractometer with a Cu Kα (λ = 1.541 78 Å) radiation source. The structural characterization was carried out using high-resolution transmission electron microscopy (HRTEM, JEOL JEM-4000EX), with an accelerating voltage of 400 kV. The sectioned specimens for the TEM imaging study were prepared from epoxy-resin-embedded metal microtubules using an ultramicrotome (Ultracut E of Reichert-Jung) equipped with a diamond knife. The produced slices, about 50 nm thick, were collected on copper grids for TEM observations. Electron spin resonance (ESR) spectra were obtained using a Bruker EMX-10 X-band (9.8 GHz) spectrometer with α,α′-diphenyl-β-picryl hydrazyl (DPPH) as the calibration reference. The conductivity measurement was performed with a standard four-in-line probe method, using a constant current source (Keithley 220) and a multimeter (Keithley 196). The conductivity data reported herein were the average values obtained for 8−10 specimens. Thermogravimetric analysis in conjunction with differential thermal analysis (TG−DTA) was performed with a Seiko Instruments model SSC5200 analyzer. Samples for TG−DTA studies were heated from 30 to 1000 °C with a heating rate of 10 °C/min using nitrogen at a flow rate of 100 mL/min.

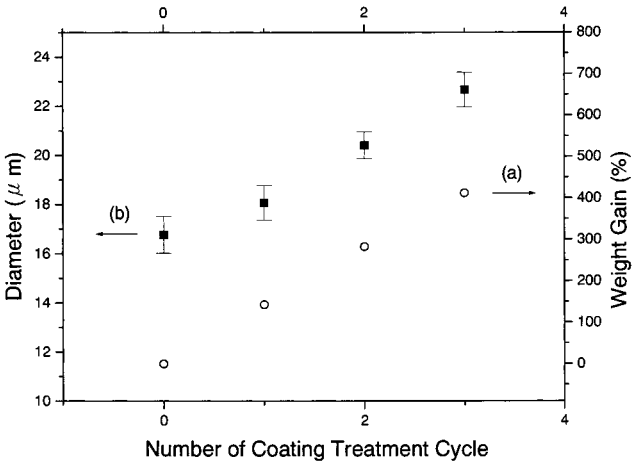

Figure 2. Outer diameter of the resultant Ni/PET composite fibers and percentage weight gains of the corresponding composite fibers (basing on the weight of the corresponding parent PET fiber) after one, two, and three cycles of electroless-plating treatment.

Results and Discussion

Formation and Characterization of Metal Microtubules. The resultant metal microtubules, as illustrated in Figure 1, were all found to be hollow tubes with uniform diameter and wall thickness. Most interestingly, distinct microtubules with an internal diameter close to that of the individual filament within the original PET yarn (containing ca. 180 filaments) were obtained. The result proved that the electroless plating was initiated and proceeded right on the surface of the individual filament. The results in Figure 2 indicated that both the weight and diameter of the resultant Ni/PET composite fibers increased with the number of plating treatment cycles. The Ni microtubules yielded from the composite fibers of the first, second, and third coating cycle were found to have an average wall thickness of 1.84 ± 0.29, 2.74 ± 0.34, and 4.27 ± 0.34 μm (Figure 1a−c), respectively. These results were consistent with the observed increase in thickness of the Ni-plating skin layer when the number of coating cycles was increased. Furthermore, Ni microtubules of different sizes can also be easily prepared with the same method using PET fibers of different diameter. For

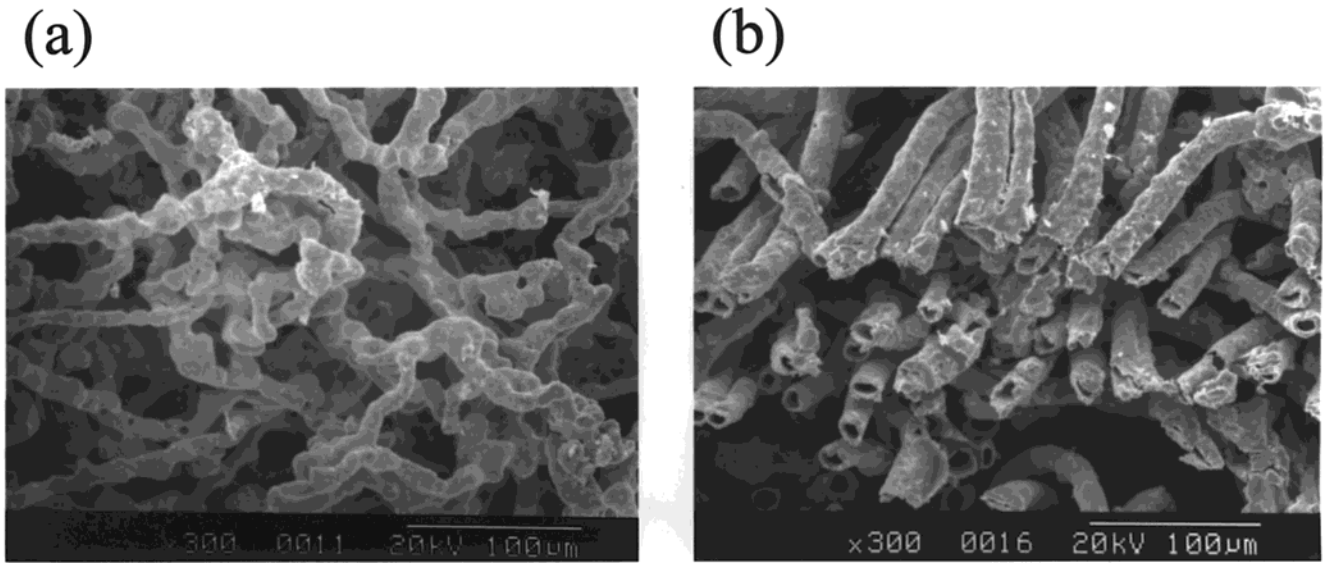

Figure 3. SEM micrographs for the Cu microtubules prepared from a Cu/PET composite fiber with five cycles of electroless-plating treatment: (a) as prepared, (b) the cross-sectioned sample of (a).

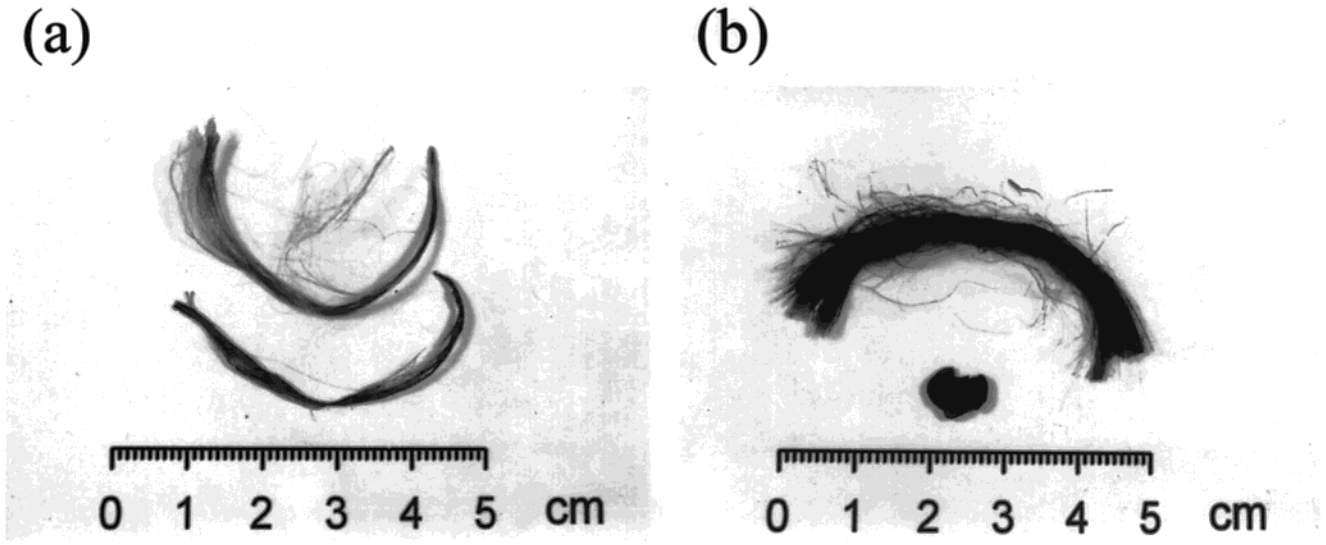

Figure 4. Photographs for (a) Ni microtubules (bottom) and their parent Ni/PET composite fibers with three cycles of electroless-plating treatment (top) and (b) Cu microtubules (bottom) and their parent Cu/PET composite fibers with five cycles of electroless-plating treatment (top).

instance, Ni microtubules with a diameter of ca. 7 μm could be prepared from PET fibers with a diameter of 7.5 μm (Figure 1e). Moreover, if the fiber loading in the plating bath (i.e., the area of the plated surface vs the volume of the plating bath) was too high, the resultant metal skin layer would not be able to completely or homogeneously cover the surface of the PET fiber, and this would result in highly fragile and easily damaged Ni microtubules. For example, when twice the amount of PET fiber was plated with the same volume of the above Ni plating solution, the resultant Ni microtubules would be mostly broken or collapsed (Figure 1f).

Similarly, Cu microtubules can also be prepared from the corresponding Cu/PET fibers (Figure 3a,b). The SEM micrograph in Figure 3b showed that all the resultant Cu microtubules were also hollow like the Ni microtubules but with the cross section being slightly distorted from circular shape (such distortion was not noticed for Ni microtubules) which was probably due to distortions of the softer metallic copper during SEM specimen preparation. Furthermore, unlike the nickel microtubules, which retained the general shape and dimensions of the parent Ni/PET composite fibers (Figure 4a), the shapes and dimensions of the resultant Cu microtubules differed dramatically from their parent Cu/PET composite fibers, as shown in Figure 4b. Further investigation with SEM showed that all of the Cu microtubules were seriously shrunk and curled (Figure 3a), with the outer diameter reduced from 23.3 $\pm$ 0.8 μm to 14.0 $\pm$ 1.4 μm and the inner diameter from 16.77 $\pm$ 0.75 μm to 8.64 $\pm$ 0.55 μm, whereas the thickness of Cu layer was also reduced from 3.39 $\pm$ 0.44 μm to 2.48 $\pm$ 0.40 μm. Such changes in dimensions for the Cu system may result from the so-called sintering process,[8] which is driven by interparticle solid-phase

(7) (a) Honma, H.; Koshio, T.; Hotta, S.; Watanabe, H. *Plat. Surf. Finish.* **1995**, *82*, *60*. (b) Baumgartner, C. E. *Plat. Surf. Finish.* **1989**, *76*, 53. (c) Shipley, C. R., Jr. *Plat. Surf. Finish.* **1984**, *71*, 92.

(8) Waldron, M. B.; Daniell, B. L. *Sintering*; Heyden & Son: London, 1978.

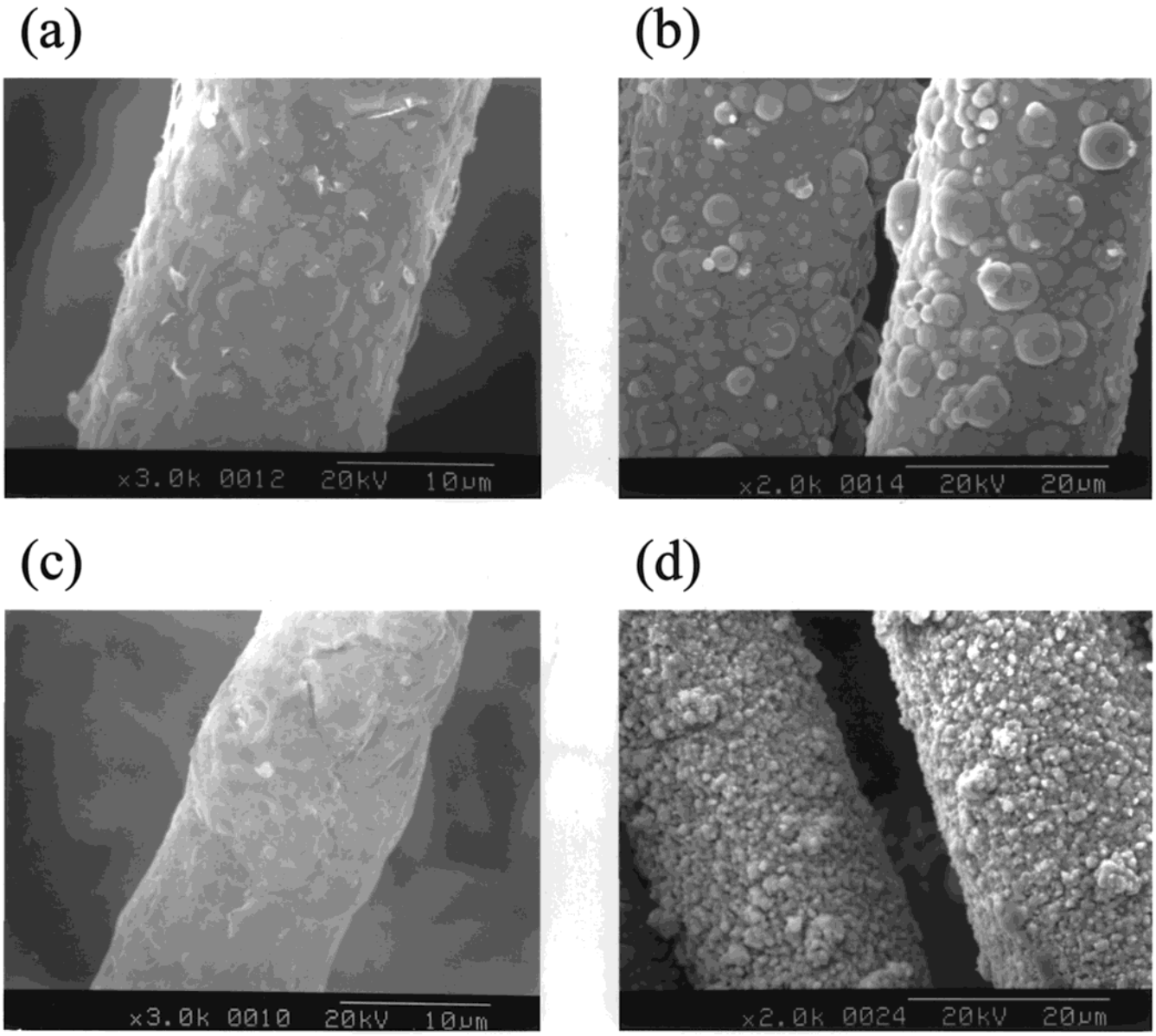

Figure 5. SEM micrographs for (a) Ni microtubules, (b) their parent Ni/PET composite fibers (with two cycles of electroless-plating treatment), (c) Cu microtubules, and (d) their parent Cu/PET composite fibers (with five cycles of electroless-plating treatment).

diffusion and often occurs at temperatures below the melting point of the materials involved. Sintering will result in volume reduction due to the elimination of excess surface area, pore shrinkage, and elimination. Such a rationale is supported by the observation that the morphology of the Cu skin layer has changed significantly during the thermal treatment process. SEM micrographs (Figure 5c,d) showed that the morphology of the Cu skin layer was converted from a loosely packed structure for the Cu/PET composite fiber (consisting of well-defined and loosely packed Cu particles) to a highly fused and continuous film-like structure, whereas the Ni skin layer of the Ni/PET composite fibers (Figure 5b) showed a rather uniform and densely packed structure with embedded nodular morphology, which was basically preserved after the thermal treatment at 800 °C (Figure 5a,b). Similar minor shrinkage (ca. 0.1%) for the Ni plating after being annealed at above 300 °C has also been observed previously.[9] Such different behaviors on morphological change between Ni and Cu microtubules can be most likely ascribed to the difference in the packing morphology of the metal skin layer, as suggested by the HRTEM images showing that the walls of Ni microtubules have a densely packed structure, while the Cu tube walls have many large cavities and pinholes.

The other possible cause may be the different sintering rate of the metal layer for coated PET fibers. Because the 800 °C treatment temperature is closer to the melting point of pure copper (1083 °C)[10] than to that of pure Ni (1453 °C),[10] the rate of sintering of a copper layer at 800 °C would be naturally expected to be much faster than that of a nickel layer.

However, such a possibility has been ruled out by our TG−DTA studies on Cu/PET and Ni/PET composite fibers, because the melting point of the Ni-plating layer

(9) Parker, K. *Plat. Surf. Finish.* **1992**, *79*, 29.
(10) *Merck index*, 12th ed.; Budavari, S., Ed.; Merck & Co., Inc.: Whitehouse Station, NJ, 1996.

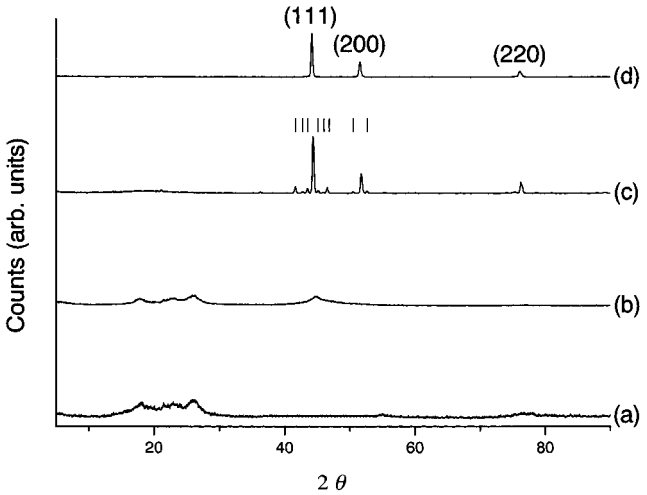

Figure 6. XRD patterns for (a) the PET fiber, (b) the Ni/PET composite fiber (with three cycles of electroless-plating treatment), (c) the ground-up powder of the resultant Ni microtubules, and (d) pure Ni powder. The diffraction peaks of Ni_3P in (c) are marked with short bars.

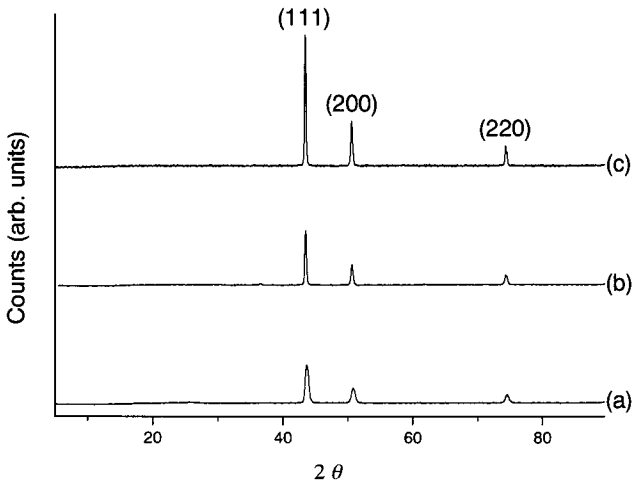

Figure 7. XRD patterns for (a) the Cu/PET composite fiber (with five cycles of electroless-plating treatment), (b) the ground-up powder of the resultant Cu microtubules, and (c) the pure Cu powder.

(896 °C) was found to be actually lower than that of the Cu-plating layer (1079 °C). The fact that the Cu-plating layer has a melting point (1079 °C) very close to that of pure Cu metal (1083 °C) suggests that the Cu-plating layer should have a composition quite similar to the pure Cu metal. In contrast, the Ni-plating layer should contain a significant amount of foreign elements (e.g., phosphorus) because of the much lower melting point of the Ni-plating layer (896 °C) than the pure Ni metal (1453 °C). Such a possibility was confirmed by the studies with X-ray photoelectron spectroscopy (XPS) and inductively coupled plasma atomic emission spectroscopy (ICP-AES); both results observed the presence of ca. 7−9 mol % of P in the Ni-plating layer, which could account for the much-lowered melting point of this layer. Similar low-melting-point (ca. 890 °C) behavior has been observed for a Ni-plating product containing ca. 8 mol % of P.[7c]

The X-ray diffraction pattern (XRD) for the ground-up Ni microtubules formed at 800 °C for 3 h (Figure 6c) showed three intense diffraction peaks at $2\theta = 44.54°$, 51.90°, and 76.56°, similar to those peaks at $2\theta = 44.54°$, 51.89°, and 76.78° for a pure Ni powder (from Fisher Scientific) measured under the same conditions (Figure 6d). The corresponding d spacing for these peaks was calculated to be 2.034, 1.762, and 1.244 Å, which is consistent with the respective d spacing for the (111), (200), and (220) planes of a fcc-Ni.[11a] Interestingly, the XRD pattern for the resultant Ni microtubules also showed several small diffraction peaks (marked with short bars in Figure 6c) at 2θ of 41.80°, 42.90°, 43.62°, 45.24°, 45.90°, 46.64°, 50.54°, and 52.70°. The corresponding d spacing for these peaks was calculated to be 2.161, 2.108, 2.075, 2.004, 1.977, 1.947, 1.806, and 1.737 Å, which is consistent with the respective d spacing for the (231), (330), (112), (240), (202), (141), (222), and (132) planes of tetragonal Ni_3P crystallites.[11b,12] Similar results have been observed previously for Ni electroless plating using the same phosphorus-containing compound of sodium hypophosphite as reducing agent.[12] It is believed that the P resulted from the possible coreduction of sodium hypophosphite with Ni(II) and presented itself in the Ni(0) matrix as a Ni−P solid solution.[13] Upon heat treatment at different temperatures, the Ni−P structure underwent crystallization to transform into crystalline Ni and various intermediate Ni_xP_y phases and completed its transformation at above 360 °C, leaving the final equilibrium mixture of crystalline Ni and Ni_3P precipitates.[12,14]

Furthermore, the results also showed that the fwhm (full width at half-maximum) for the Ni(111) peak has been significantly reduced from 2.51° (for the Ni/PET composite fiber) to 0.30° (for the Ni microtubules), confirming the increase of the average crystallite size, L_{111}, from ca. 34.5 to 932.0 Å (estimated according to Scherrer's equation[15]) during the thermal annealing process.

The XRD pattern for the ground-up Cu microtubules (Figure 7b) also showed three intense diffraction peaks at $2\theta = 43.33°$, 50.49°, and 74.15°, similar to those peaks (at $2\theta = 43.33°$, 50.47°, and 74.19°) for a pure Cu powder (from Wako) measured under the same conditions, as displayed in Figure 7c. The corresponding d spacing for these peaks was calculated to be 2.088, 1.807, and 1.279 Å, which is consistent with the respective d spacing for the (111), (200), and (220) planes of a fcc-Cu.[11c] Furthermore, the fwhm (full width at half-maximum) for the Cu(111) XRD peak was reduced from 0.65° (for the Cu/PET composite fiber) to 0.27° (for the Cu microtubules), confirming the increase of the average crystallite size, L_{111}, from ca. 160.3 to 544.7 Å (estimated according to Scherrer's equation[15]) during the thermal annealing process.

To understand the structure in further details, the cross-sectioned specimens (ca. 50 nm thick) prepared

(11) (a) *PCPDFWIN*, version 1.30; JCPDS X-ray Powder Data File No. 04-0850; 1997. (b) *PCPDFWIN*, version 1.30; JCPDS X-ray Powder Data File No. 34-0501; 1997. (c) *PCPDFWIN*, version 1.30; JCPDS X-ray Powder Data File No. 04-0836; 1997.

(12) Yamamoto, M.; Shirai, K.; Watanabe, N. *J. Electrochem. Soc.* **1991**, *138*, 2082.
(13) Spencer, L. F. *Met. Finish.* **1974**, *72*, 35.
(14) Agarwala, R. C.; Ray, S. *Z. Metallkd.* **1989**, *80*, 556.
(15) Chung, D. D. L.; DeHaven, P. W.; Arnold, H.; Ghosh, D. *X-ray Diffraction at Elevated Temperatures: A Method for In Situ Process Analysis*; VCH Publishers: New York, 1993.

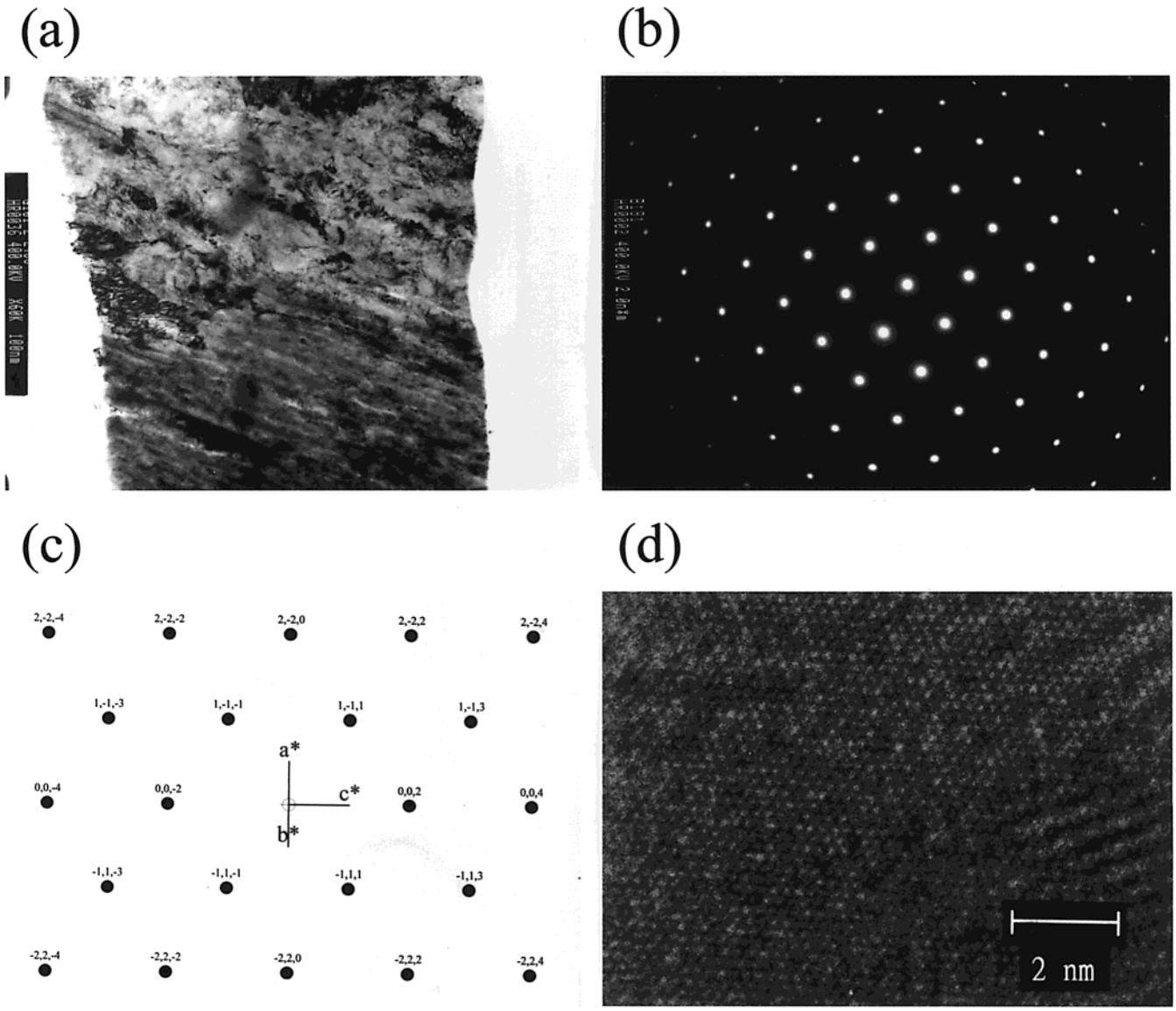

Figure 8. HRTEM results of Ni microtubules: (a) image of a cross-sectioned sample specimen of the Ni microtubule (ca. 16 μm in diameter) of Figure 1c; (b) selected area electron diffraction pattern for the center area of (a); (c) simulated image for a fcc-Ni phase with computer program CaRIne Crystallography v3.1; and (d) lattice image of the specimen in (a).

from the epoxy-resin-embedded metal microtubules using an ultramicrotome were inspected with high-resolution transmission electron microscopy (HRTEM). The HRTEM studies showed that Ni microtubules have a densely packed structure with little void spaces (Figure 8a). The selected area electron diffraction (Figure 8b) recorded for the same specimen of Ni microtubules showed a diffraction pattern consistent with that of a single-crystal fcc-Ni[16] with the [110] zone axis perpendicular to the cross section of the microtubules. Furthermore, the image simulation for a fcc-Ni phase, as performed with the computer program CaRIne Crystallography v3.1 (Figure 8c), also showed a well-matched diffraction pattern. Indexing the diffraction pattern revealed that the Ni microtubules were grown predominantly along the [110] direction, with some Ni_3P crystalline precipitates (ca. 6 nm $\times$ 10 nm in size) sparsely dispersed within the Ni matrix. Figure 8d shows a lattice image of the tube wall as viewed from the longitudinal axis of the Ni microtubules.

The HRTEM studies for Cu microtubules however showed a very different structural feature. The image in Figure 9a for a cross-sectioned slide (ca. 50 nm thick) of Cu microtubule shows many large cavities and pinholes were present within its tube wall. The selected area diffraction pattern in Figure 9b clearly indicates that the Cu microtubules are polycrystalline in structure.

The anisotropic orientation nature of Ni microtubules has also been confirmed by the electron spin resonance (ESR) studies. The results in Figure 10 indicated that the ground-up powder of Ni microtubules revealed an ESR spectrum similar to that of pure Ni powder (Figure 10a and 10b), whereas the Ni microtubules, in the form of a microtubular bundle with the tube axis being perpendicular to the applied magnetic field, showed very different spectral features (Figure 10c) than the ground-up powder sample. A control study using the same Ni microtubular bundle with the tube axis being parallel

(16) (a) Mai, Q. X.; Daniels, R. D.; Harpalani, H. B. *Thin Solid Films* **1988**, *166*, 235. (b) Jankowski, A. F.; Wall, M. A. *J. Mater. Res.* **1994**, *9*, 31.

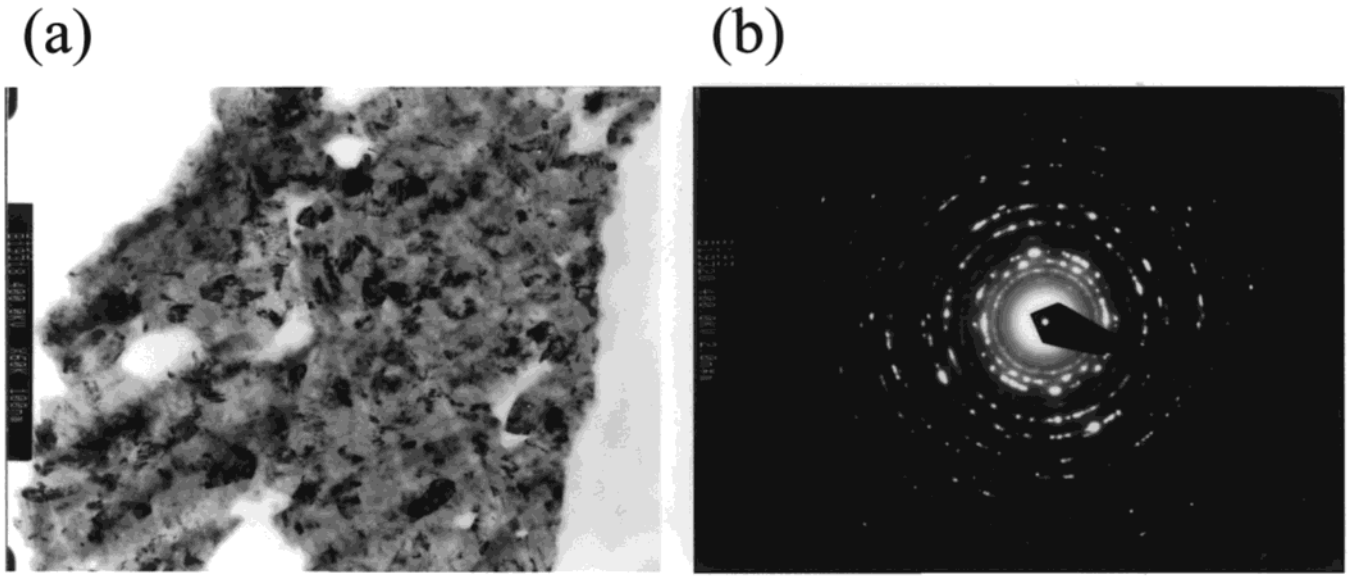

Figure 9. HRTEM results of Cu microtubules: (a) image of a cross-sectioned sample specimen of the Cu microtubule (ca. 14 μm in diameter) of Figure 3; (b) selected area electron diffraction pattern for the center area of (a).

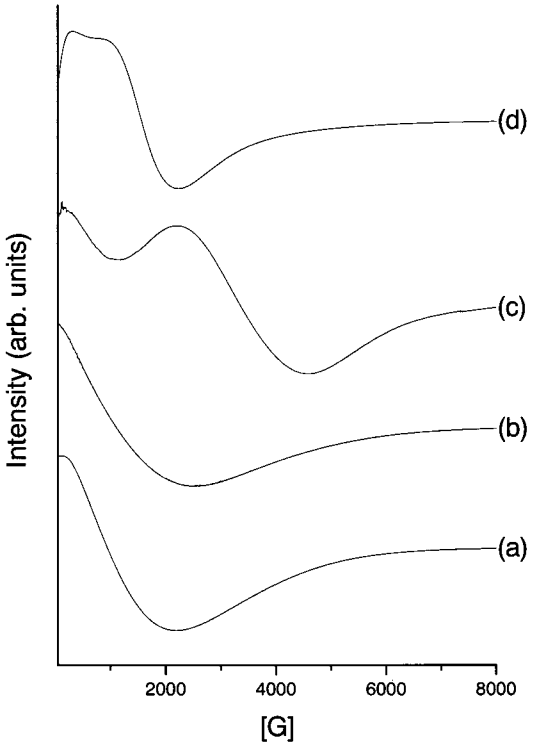

Figure 10. ESR spectra for (a) pure Ni powder, (b) ground-up powder of Ni microtubules, and Ni microtubular bundles with the tube axis being perpendicular (c) or parallel (d) to the applied magnetic field.

to the applied magnetic field also showed a very different ESR spectral feature (Figure 10d) from that of the perpendicular sample, confirming that the magnetic crystallites within the Ni microtubules are indeed preferentially oriented along the direction. A similar anisotropic magnetic property for the Ni microtubules prepared with the microporous polycarbonate templates has also been previously observed with SQUID (superconducting quantum interference device magnetometer).[17]

Furthermore, the conductivity of these metal microtubules and their corresponding metal/PET composite fibers was studied with a typical four-in-line probe method. The conductivity of Cu/PET and Ni/PET composite fibers was measured to be 1.58×10^5 ($\pm$25%) S/cm and 8.95×10^3 ($\pm$22%) S/cm, respectively. The lower conductivity of the Ni/PET composite fiber may be attributed to the small Ni crystallite size and the presence of a large amount of P inclusions in the Ni-plating layer. Interestingly, the conductivity of the Ni microtubules was found to have significantly increased to 1.22×10^5 ($\pm$20%) S/cm, which is very close to the conductivity of 1.5×10^5 S/cm for pure Ni metal.[10] The enhanced conductivity of the Ni-layer after the thermal treatment may be ascribed to the increased Ni grain size (which would lead to the reduction in grain surface energy), the exclusion of P from the crystalline Ni phase as NiP_3 precipitates, and the enhanced orientation order of Ni crystallites. As for the Cu microtubules, although their conductivity cannot be conveniently measured due to their serious shrinkage and distortion in shapes during the annealing treatment, their conductivity is expected to be higher than that of the parent Cu/PET composite fibers, judging from the fact that the crystallite size of Cu plating has also significantly increased after the thermal annealing treatment.

Formation of Well-Organized Metal Microtubule Structures. The current method also enables the preparation of three-dimensionally assembled Ni microtubules. For example, three-dimensionally weaved Ni microtubules can be prepared by thermal annealing a twice-plated Ni/PET cloth at 800 °C for 3 h under N_2 flow (at 0.5 L/min) in a quartz tube oven. Similarly, bundles of Ni microtubules have also been prepared from the bundles of Ni/PET composite fibers. All of the Ni microtubules within these regularly assembled structures are found by SEM to be hollow. Thus, this method enables the preparation of various well-organized metal-tube structures via the use of predesigned woven templates, which would provide a convenient and

(17) Whitney, T. M.; Jiang, J. S.; Searson, P. C.; Chien, C. L. *Science* **1993**, *261*, 1316.

feasible approach for designing and fabricating actual articles or devices for various practical applications.

Conclusions

Through the use of the method reported herewith, Ni microtubules with essentially single crystalline structure and Cu microtubules of polycrystalline nature have been successfully prepared. Interestingly, although the employed PET yarn contains ca. 180 filaments in each bundle, the resultant metal microtubules were found to have a size that resembled the individual filament instead of the whole PET yarn. The result strongly suggested that the electroless plating initiated and proceeded right on the surface of the individual filament. Hence, this method provides a convenient, high-throughput approach for making metal microtubules without the need for separating and handling of individual PET filaments with rather complicated devices and/or expensive facilities as reported in other studies.[1o] Although the current study is focused on micrometer-sized metal-tubes, it is envisaged that such a preparation method will also be applicable for similarly prepared nanometer-sized metal tubes, if the recently developed nanometer-sized fibers[18] are available.

Acknowledgment. We acknowledge the financial support from National Science Council.

CM0103287

(18) Kageyama, K.; Tamazawa, J.-I.; Aida, T. *Science* **1999**, *285*, 2113.